

**Silica as a Model Ice-Nucleating Particle to Study the Effects of Crystallinity, Porosity and  
Low-Density Surface Functional Groups on Immersion Freezing**

Katherine E. Marak<sup>1</sup>, Julian H. Roebuck<sup>1</sup>✉, Esther Chong<sup>1</sup>✉, Haley Poitras<sup>1</sup>✉, Miriam Arak

Freedman<sup>1,2,\*</sup>

*1) Department of Chemistry and 2) Department of Meteorology and Atmospheric Science*

*The Pennsylvania State University, University Park, PA 16802, USA*

Revision Submitted to *Journal of Physical Chemistry*

*August 15, 2022*

\* To whom all correspondence should be addressed: [maf43@psu.edu](mailto:maf43@psu.edu)

✉ Present address: Boston University, Boston, MA 02215

✉ Present address: Sun Pharmaceuticals, Billerica, MA 01821

✉ Present address: National Ground Intelligence Center, Charlottesville, VA 22911

**Abstract:**

Aerosol particles can facilitate heterogenous ice formation in the troposphere and stratosphere by acting as ice-nucleating particles, modulating cloud formation/dissipation, precipitation, and their microphysical properties. Heterogeneous ice nucleation is driven by ice embryo formation on the particle surface, which can be influenced by features of the surface such as crystallinity, surface structure, lattice structure, defects, and functional groups. To characterize the effect of crystallinity, pores, and surface functional groups towards ice nucleation, samples of comparable silica systems, specifically, quartz, ordered and non-ordered

porous amorphous silica samples with a range of pore sizes (2-11 nm), and non-porous functionalized silica spheres were used as models for mineral dust aerosol particles. The ice nucleation activity of these samples was investigated using an immersion freezing chamber. The results suggest that crystallinity has a larger effect than porosity on ice nucleation activity, as all of the porous silica samples investigated had lower onset freezing temperatures and lower ice nucleation activities than quartz. Our findings also suggest that pores alone are not sufficient to serve as effective active sites, and need some additional chemical or physical property, like crystallinity, to nucleate ice in immersion mode freezing. The addition of a low density of organic functional groups to non-porous samples showed little enhancement compared to the inherent nucleation activity of silica with native surface hydroxyl groups. The density of functional groups investigated in this work suggests that a different arrangement of surface groups may be needed for enhanced immersion mode ice nucleation activity. In summary, crystallinity dictates the ice nucleation activity of silica samples rather than porosity or low-density surface functional groups. This work has broader implications regarding the climate impacts resulting from ice cloud formation.

## **Introduction:**

Heterogeneous ice nucleation is a significant mechanism of ice nucleation in the troposphere and the stratosphere.<sup>1-4</sup> Heterogenous surfaces can lower the activation energy for water to nucleate and freeze and therefore raise the ice nucleation temperature compared to that of homogenous aqueous droplets.<sup>1</sup> The heterogeneous interactions between a surface and water at the interface is influenced by the structure of the surface, the contact angle and the energetics

of the surface.<sup>5</sup> Heterogeneous ice nucleation is also a subject of interest in materials science, agriculture, food science, and other disciplines.<sup>5-8</sup>

Heterogenous ice formation in the troposphere is complex and several pathways of heterogenous freezing have been proposed, including contact freezing, deposition mode/pore condensation freezing, condensation freezing, and immersion freezing, with the latter being the one explored in this work.<sup>9,10</sup> Immersion freezing involves a solid particle (CCN) suspended in liquid water that catalyzes ice nucleation. For cirrus clouds and mixed phase stratiform clouds, heterogeneous immersion freezing has been proposed to be the dominant method for ice formation.<sup>11,12</sup> In this mechanism of ice nucleation, the ability of the particle to order water in solution is the most significant factor. Interactions at the surface-water interface can result in ordering of water into pre-ice clusters which enhance ice nucleation activity.<sup>13,14</sup> However, not every aerosol particle is equally active as an ice-nucleating particle, and indeed materials with the same composition but different surface morphology can have different freezing efficiencies.<sup>2,15</sup> Therefore, a greater look into which active sites initiate nucleation and freezing is necessary. Crystal structure, lattice spacing, crystallinity, surface defects (pores, ridges, etc.), composition, and surface functional groups can all contribute to the ice nucleation activity of a particle.<sup>16-21</sup>

Ice formation at the surface of a particle happens at specific sites often referred to as active sites, however there are a variety of surface features that could induce ice nucleation. Recent work combining high-speed imaging with optical or electron microscopy has shown that distinct sites in both immersion and deposition mode freezing are responsible for initiating ice nucleation.<sup>19-22</sup> These sites have been shown to mostly occur at physical features like surface defects or pores on the surface of the minerals investigated.<sup>22,23</sup> However, other features of the

surface such as crystallinity, lattice spacing, and functional groups, are important for the observed ice nucleation behavior as well.<sup>18,23-25</sup>

The role of pores in heterogeneous ice nucleation is an area of current focus in the literature. In particular, it has been proposed that what is observed as deposition mode freezing is actually homogeneous or immersion freezing of water trapped within pores and grooves and this phenomenon has been termed pore condensation.<sup>26-29</sup> Wagner et al. demonstrated the enhancing effects that supercooled and frozen water in pores had on the ice nucleation of porous materials like diatomaceous earth and zeolites.<sup>30</sup> Pore sizes in mineral dust samples vary greatly, with illite samples having small pores around 10Å and kaolinite samples having pores around 30nm.<sup>31,32</sup> Effects of nanoconfinement of water in both pores and grooves have shown enhancement of ice nucleation for a large range of sizes (0.98-8 nm), depending on the material.<sup>30,32-35</sup> Some microscopy studies also give evidence that pores play a large role in deposition mode freezing.<sup>36</sup> The microscopy investigation, however, was on large pores (1-5  $\mu$ m), which does not rule out some physical or chemical feature within the pore that may have promoted ice nucleation.<sup>36</sup> Additionally, the ice nucleation of carbon nanotubes has been investigated by our research group and others as a model for porous carbon-based aerosols.<sup>32,37</sup>

In the atmosphere, mineral particles have exposed functional groups at the surface, often containing oxygen, with the simplest and most common for mineral dust being hydroxyl (OH) groups. It is possible for these exposed groups to create a charge on the surface which have been shown to influence the density of water at the surface and the freezing temperature.<sup>38,39</sup> Negative charged surfaces tend to inhibit ice nucleation, while positive surfaces tend to promote ice nucleation.<sup>39-42</sup> In addition, heterogenous chemistry, such as oxidative reactions, can occur and cause a variety of functional groups to be present on the surface of an aerosol particle. Hydroxyl

groups on the surface have a complex effect on ice nucleation activity, and have been demonstrated to both impede and enhance this activity.<sup>6,24,43</sup> In simulations, a combination of factors, like increased OH group density on features like step edges and interaction of the substrate and water are more important than the number and arrangement of OH groups alone.<sup>43,44</sup> For iron oxide particles, Chong et al. demonstrated that a combination of lattice match and increased OH group density was more important for ice nucleation activity than either factor alone.<sup>24</sup>

Surfaces (liquid or solid) coated in or functionalized with hydrocarbons show that ice nucleation activity is dependent on a variety of factors including chain length, rigidity, and functional groups. For example, increasing hydrocarbon chain length for long-chain alcohols at the air-water interface raises the freezing point temperature and contributes to the increased ordering of these surface groups.<sup>45,46</sup> Both modelling work and laboratory studies of long chain alcohols and carboxylic acids have been performed in which the surface organic compounds are a well-ordered monolayer of ligands ( $\approx 5.4$  groups per square nanometer) and these studies suggest that alcohols are more active than carboxylic acids at nucleating ice.<sup>46,47</sup> Carboxylic acids are expected to be less active than alcohols because they have stronger interactions with adsorbed water, limiting the ability of the surface to template water for ice formation.<sup>6</sup> Additionally, the effectiveness of alcohols has been attributed to structural fluctuations at the surface which allow the alcohol to have a greater lattice match to ice.<sup>46,48,49</sup> A comparison between perflourinated organic acids (PFOA) and aliphatic acids of the same chain length show an increase in freezing temperature attributed to the added rigidity of the perflourinated acids.<sup>40</sup> However, coatings of this kind are not as effective at nucleating ice until there is at least a monolayer at the surface.<sup>40</sup> For example, Pluhařová et al. has found that homogeneous freezing is

affected by the presence of submonolayer concentrations of pollutants like pentanol and pentanoic acid on the surface of water with the alcohol inhibiting ice formation and the acid causing no change.<sup>50</sup> Additionally, for functional groups on solid surfaces, work performed on self-assembled monolayers with a mixture of CH<sub>3</sub> and OH terminated alkyl chains (number of carbon atoms = 9 to 21) on gold has shown that decreasing carbon chain lengths can decrease the surface ordering and therefore also decrease hydrophilicity.<sup>51,52</sup> In contrast to studies of the effect of surface functional groups, recent experimental work has found evidence that organic coatings do not play a significant role in IN activity for immersion mode freezing and may have a slight inhibition effect by covering surface active sites.<sup>16,53</sup>

Silica is a good model system for mineral dust particles in the atmosphere because silica is one of the most abundant compounds on Earth and exists in both crystalline and amorphous forms.<sup>4,54</sup> Silica content has been linked to ice nucleation activity in both dust samples and volcanic ash samples, with the former effects seen below 245K.<sup>55,56</sup> The ice nucleation activity of some quartz and amorphous silica samples have been explored, although effects of porosity and crystallinity have not been directly compared.<sup>21,33,37,55,57–60</sup> Harrison et al. created a parameterization for quartz by testing several varieties and showing natural variation in crystalline quartz, with Bombay chalcedony (microporous) standing out with high activity, although the direct cause of its enhancement has not been proven.<sup>60</sup> Silica can be found in both crystalline and amorphous forms in the environment, and synthetically in the lab, it can have a variety of pore structures and can be easily functionalized.

In this paper, we aim to isolate and compare the variables of crystallinity, porosity, and surface functional groups on immersion mode freezing using silica as a model system. Four silica samples with pore sizes ranging from 2-11 nm, quartz, and non-porous silica spheres were used as

model systems with controlled surface features of porosity and crystallinity. Milled quartz was selected as a highly crystalline sample to compare with amorphous non-porous silica spheres. All of the samples were used with their native surface functionalization, with the exception of non-porous spheres that were functionalized with silane chemistry. The non-porous silica spheres were functionalized to generate low density ( $\approx 1.6$  groups per square nanometer) functionalized particles. The functional groups of interest are the ones containing oxygen groups with a variety of carbon oxidation states to mimic the effects of heterogeneous atmospheric chemistry. Other functional groups were used, including amines and amides, to compare the effects of nitrogen to oxygen in the surface functional groups. These samples were investigated in an immersion freezing chamber for ice nucleation activity.

## **Methods:**

### **Materials**

Nonporous spherical silica particle-powders without surfactants (Glantreo Ltd) with diameters of 0.5, 0.75, and 1.0  $\mu\text{m}$  and a monodispersity of 8% were used as model non-porous aerosol. Ordered porous silica samples used were: MCM-41, MCM-48 and SBA-15 (ACS Chemicals). Non-ordered porous silica (Sigma Aldrich), synthesized from a modified Stöber method to allow for porosity, were also investigated.<sup>61</sup> Quartz was sourced from Ward's Natural Science Establishment and the sample is from Minas Gerais, Brazil (49-5886). The quartz was milled to 20 $\mu\text{m}$  mesh as well as milled using a McCrone micronizing mill to  $<1\mu\text{m}$  and remained crystalline as seen from a representative X-ray diffractogram (Fig S4). The ice nucleation and freezing of all of these silica samples was determined using an immersion freezing chamber. The silanes (Gelest) for silica functionalization were used with further purification:

acetoxytriethoxysilane (95%, AETS), 2-(carbmethoxy)ethyltrimethoxysilane (95%, 2-CMETS), 3-(trihydroxysilyl)-1-propane-sulfonic acid (35% in water, 3TPSA), hydroxymethyltriethoxysilane (50% in ethanol, HMT), (3-acetamidopropyl)trimethoxysilane (>95%, AAPT), triethoxysilylpropylmaleamic acid (90%, TPMA), and (3-aminopropyl)triethoxysilane (>95%, ATPES).

### Functionalized Silica Synthesis

The methods for surface functionalization of silica are well established and involve suspending the silica particles in an organic solvent (ethanol or DMF) under a nitrogen atmosphere and adding excess of the desired triethoxysilane (Gelest),  $X\text{-Si(OCH}_2\text{CH}_3)_3$ , dropwise and refluxing for 6 hours or stirring for 24 hours at room temperature. The reaction mixture is then centrifuged three times in water to remove excess starting material.<sup>62,63</sup> The reactions were performed at room temperature in ethanol.

For these syntheses, one of the desired surface groups replaces three hydroxyl groups at the surface as they react with the triethoxysilyl group to displace ethanol, as seen in Figure 1. Typically amorphous silica has between 4.6-4.9 OH groups per nm on the surface which would result in approximately 1.6 organic functional groups per nm on the surface of these particles when functionalized.<sup>57,64,65</sup> However, it is possible that the silanes react with one another and this can complicate the picture of functional group density on the surface. The synthesis method involved dropwise addition of silane. The small quantities involved in the synthesis and the estimation of surface hydroxyl groups made exact stoichiometric amounts impossible.

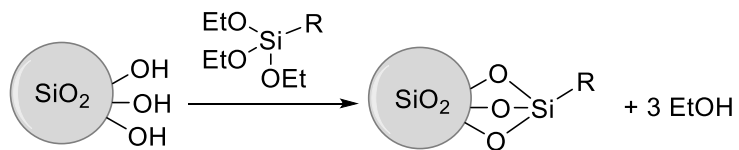


**Figure 1:** Synthetic scheme for surface functionalization of a silica particle (gray, not to scale) where three surface hydroxyl groups are replaced by the silane with desired functionality and ethanol is displaced.

### Characterization of Samples

**TGA-MS:** A Discovery Series TGA Q5500 coupled with a Discovery MS was used to approximate the amount of each organic group that was added to the surface of the 1.0  $\mu\text{m}$  non-porous silica particles during silanization. The mass spectrometer measures several molecular weights during the course of the TGA run. As a result, several species of interest were monitored, including desorption of gasses like water and  $\text{CO}_2$  at low temperatures and the decomposition of the organic functional group. The weight percent change occurring with decomposition of the organic function group was used to calculate the theoretical conversion of surface OH groups to organic surface groups. The coupled Discovery MS was used to confirm that the mass fragments lost while heating corresponded to the organic functional groups that were added to the silica surface.

**BET:** Brunauer-Emmet-Teller (BET) analysis was performed with nitrogen gas using an ASAP 2020 Automated Surface Area and Porosimetry System (ASAP) 2000 to determine the surface area of each sample. Each sample in its powder form is degassed at 90 °C under a vacuum for 2 hours prior to being analyzed. Error in the measurements is calculated by deviation in repeat measurements. The BET surface area of the bare silica particles was used in calculations for the functionalized particles, which assumes that the size of the particle does not change significantly with functionalization. Generally, only a monolayer of the silane is added, and as a result, this assumption should be reasonable. However, TGA-MS of three samples, 3TPSA, HMT and

ATPES, indicated there may be more than a monolayer present at the surface and as a result individual BET surface areas were measured for these samples.

## IN Chamber

The immersion chamber is shown in Figure 2, and was first described by Alstadt et al.<sup>32</sup> The chamber is a copper block housed inside of an aluminum frame with two optical cast plastic windows on the top and bottom. Nitrogen gas is passed through a copper coil that is submerged in liquid nitrogen and then enters the chamber and flows through the copper block at a controlled rate of -3°C/minute using a rotameter. A K-type thermocouple is used to monitor the temperature of the copper block and is attached near to where the siliconized (hydrophobic) glass slide is placed for the most accurate temperature reading. There are polyimide heaters attached to the sides of the copper block which allow us to end a trial and bring the chamber back to room temperature for the next trial. The chamber has a purge flow of nitrogen gas to prevent water vapor from condensing inside. The flow of nitrogen is not strong enough to noticeably evaporate the particles during the duration of the trial (~ 10 min). Above the chamber is a CCD camera and a light to capture an image of the droplets at every 0.5 °C.

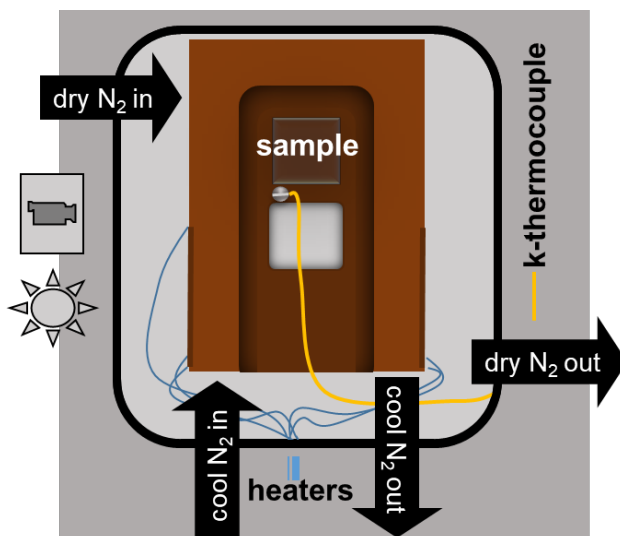


**Figure 2:** Schematic of immersion ice nucleation chamber

## Ice Nucleation Trials

The silica particles are suspended in 0.03 micron filtered UHPLC water (Thermo Scientific) at 0.02%w/v by sonication for 10 minutes. It has been established by TEM that this duration of sonication has no visible effect on the surface since the particles remain smooth and there are no obvious defects (not shown). For each sample, at least 100 2  $\mu$ L drops of the suspension are tested for their ice nucleation activity in the chamber described above. To achieve this, typically 4 trials of 30 particles are analyzed for each suspension. For each particle type, at least two different suspensions are tested. The average number of particles in a droplet is on the order of  $10^4$  particles per sample and varies slightly depending on the particle size distribution. Particle concentrations of this magnitude are within previous literature ranges for droplets of this size.<sup>32</sup>

The activity of the particles was evaluated using frozen fraction, which is indicative of ice nucleation activity. Frozen fraction,  $F(T)$ , is calculated as  $n(T)/N$ , where  $n(T)$  is the number of droplets frozen at a given temperature and  $N$  is the total number of droplets. Frozen fraction can be used to calculate  $K(T)$  which is the number of nucleation sites at a given temperature per mL as outlined by O'Sullivan<sup>66,67</sup>

$$K(T) = \frac{-\ln(1-F(T))}{V} \times d \quad (1)$$

where  $V$  is the volume of the drop in mL and  $d$  is the dilution factor.  $K(T)$  is calculated for all the trials and for the background freezing of Millipore water.

From  $K(T)$  the active sites per unit area for ice nucleation can be described by

$$n_s = K(T) \times C^{-1} \quad (2)$$

which is independent of differences in surface area of the particles and the  $K(T)$  of each trial has been corrected for background water freezing by subtracting  $K(T)_{water}$  from  $K(T)_{trial}$ .  $C$  is the total surface area in a given volume and is calculated using BET surface area and the mass percent of the silica particles in each experiment.

The standard deviation for  $n_s$  is calculated by comparing all trials of the same material. In many cases the background freezing of water is comparable to our amorphous silica samples, and as a result, the  $n_s$  is low and the deviation is high, resulting in large error which is accentuated in the log-scale.

## **Results and Discussion:**

The objective of this work is to understand how crystallinity, porosity, and low-density, non-ordered functional surface groups impact the activity of heterogeneous ice-nucleating particles using silica as a model system. The BET data of several porous samples, one non-porous sample, and a crystalline quartz sample are summarized in Table 1. One of the porous samples, which we are designating as P-Si, does not have an ordered pore structure, while both MCM and the SBA sample have well-ordered pore structures. Figure 3a shows the frozen fraction of all the silica samples investigated. Only quartz, the crystalline sample, has significant ice nucleation activity. The quartz sample ( $<20 \mu\text{m}$ ) begins freezing at  $-12^\circ\text{C}$  and is 50% frozen at  $-19^\circ\text{C}$ , which agrees with literature.<sup>21,60,68</sup> It is important to note that both of our quartz samples were milled which may add active sites.<sup>15,24</sup> However, our data are in good agreement with immersion freezing temperatures of droplets on natural facet unpolished quartz which began freezing at  $-12.7^\circ\text{C}$  and had a mean freezing temperature of  $-20.3^\circ\text{C}$ .<sup>21</sup> Additionally, Kumar et al. shows that even when in water, as long as a new silica layer has not grown, the IN activity of milled quartz remains

constant.<sup>57</sup> All other samples, porous and non-porous, are marginally more active than the baseline freezing of water. The least enhancement can be seen with the non-ordered porous sample which begins freezing at -18.5 °C and is 50% frozen at -25.3°C. This sample has a random distribution of pores and the smallest pore size at 2.0 nm which may suggest that this size combined with the random distribution of pores results in low activity towards ice nucleation, as seen in other porous mineral samples of diatomaceous earth and NX illite.<sup>30</sup> P-Si also has a large specific surface area, and despite more area for potential active sites, it has the least. In agreement with our data, it has been shown previously that amorphous silica has a limited enhancement of ice nucleation over the homogeneous freezing of water.<sup>33,57,58,69</sup> Smaller non-porous amorphous silica samples were also investigated and are shown in Fig. S1. Results for these samples were similar to background water freezing or similar to 1.0  $\mu\text{m}$  diameter silica, and therefore, 1.0  $\mu\text{m}$  were used for functionalization.

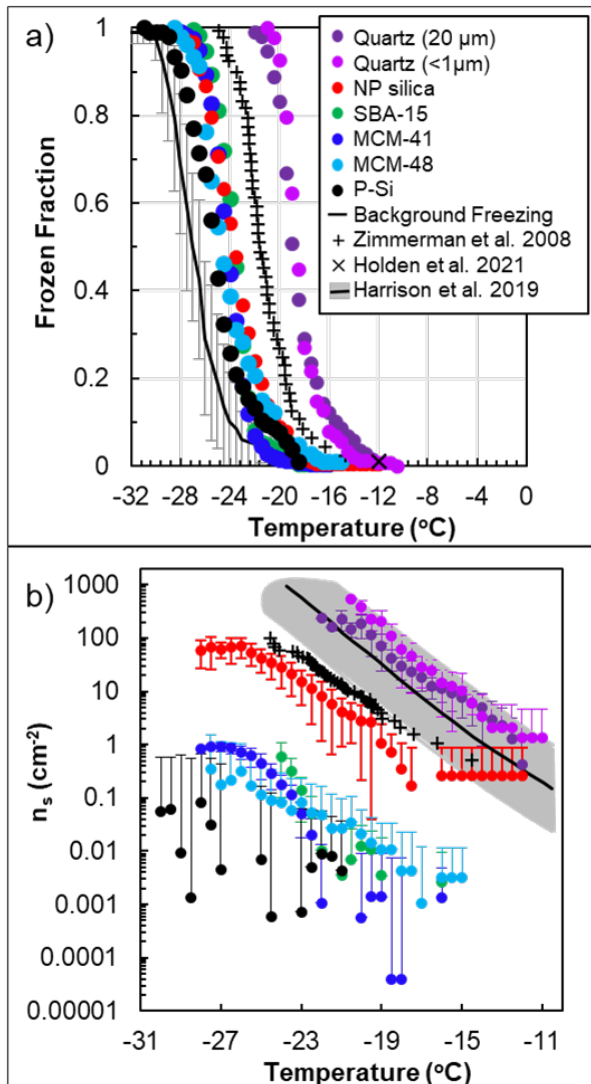


**Figure 3:** a) The frozen fraction of each silica sample at a given temperature. The error is shown for background freezing as the standard deviation between trials. b) The  $n_s$  data for each silica sample at a given temperature with the background contribution from water freezing subtracted. Both graphs use the same legend.

The BET surface area is used to normalize the frozen fraction results and convert to a plot showing active sites,  $n_s$ , as a function of temperature (Figure 3b; Table 1). Results do not show a monotonic increase in  $n_s$  with decreasing temperature due to the subtraction of background water

freezing results. Lower error bars are not present on all data points as they would fall below zero which cannot be plotted on a log scale, however they are equivalent in size to the positive error bars shown. Although the temperature dependent frozen fraction for all the amorphous samples is similar, the porous samples have more surface area than the non-porous silica spheres, resulting in fewer active sites per  $\text{cm}^{-2}$ . This result is unexpected as confined spaces like nanogrooves with widths comparable to the hexagonal ice lattice, or 1.0 and 1.7 nm have been theorized by modelling to enhance ice nucleation activity by selectively orienting water in such a way that ice formation is favorable at 220K.<sup>23,35</sup> Pre-activation of ice nucleators by ice in pores have also been seen as warm as 260K for deposition studies.<sup>30</sup> Nanoscale features like pores and step edges have also been observed via microscopy to enhance ice nucleation activity in both deposition and immersion modes, though direct correlation to porosity cannot be made with this technique.<sup>20,22,36</sup> Once again, it is clear that the quartz sample is the most active, as it has the most active sites at every temperature. Our data for quartz fall in the range of other mineral dust samples, as expected from the literature, making it a decent model for mineral dust.<sup>4,58,60,68,70</sup> Additionally, both milled quartz samples fall in line with the quartz parameterization laid out by Harrison et al.<sup>60</sup> These data suggest that crystallinity of a sample is more important than porosity as it pertains to immersion freezing. Crystallinity has been shown in other samples to be a significant factor, separate from the lattice spacing and crystal geometry.<sup>18</sup> Porosity has mainly been studied experimentally in deposition mode nucleation.<sup>26,27,30</sup>

**Table 1.** Characterization of Silica Samples

Silica Sample	Particle size ( $\mu\text{m}$ )	Avg Pore Size (nm)	BET Surface Area ( $\text{m}^2/\text{g}$ )
Quartz	<20	-	<b><math>3.01 \pm 0.05</math></b>
Quartz	<1	-	<b><math>1.46 \pm 0.02</math></b>

<b>MCM-48</b>	<b>0.2-0.4</b>	<b>2.7</b>	<b>333 ± 2</b>
<b>MCM-41</b>	<b>0.1-1.0</b>	<b>3.4</b>	<b>650 ± 30</b>
<b>SBA-15</b>	<b>1.0-4.0</b>	<b>6-11</b>	<b>488.4 ± 0.9</b>
<b>Non porous silica</b>	<b>1.0</b>	<b>-</b>	<b>13.14 ± 0.01</b>
<b>Porous silica, P-Si</b>	<b>1.0</b>	<b>2</b>	<b>628 ± 7</b>

Several functional groups have been added to the surface of the 1  $\mu\text{m}$  silica particles using the method described for ATPES functionalization from the literature (Table 2).<sup>62,63</sup> After functionalization, the particles were tested using TGA-MS to determine if the functionalization was successful by comparing the mass percent change of the organic decomposition to the theoretical number of OH groups on the surface. The results suggest the functionalization for all of the groups was successful, although some groups had greater than 100% yield. Silanes are able to react not only with the surface OH groups of silica, but also with other silanes in solution. Although steps in the reaction methods were taken to limit silane-silane reactivity, silane-silane reactions are likely the cause of yields greater than 100% (Table 2). For these samples, BET was measured directly rather than using the BET surface area of bare silica to account for the increase in surface area with abundant silane-silane surface reactions.

An example of a TGA spectrum for functionalized and unfunctionalized silica particles is shown in Figure 4. TGA coupled with mass spectroscopy allows us to track specific masses of interest as the sample is heated, these masses were different for each ligand investigated. As expected, the mass curve for ATPES functionalized silica shows a greater overall mass percent lost than the bare silica particles as well as a decomposition feature around 500°C indicative of the decomposition of surface groups. Both samples have a similar desorption feature starting upon initial heating (<150°C), indicating comparable levels of adsorbed water and other gasses

typically adsorbed to the surface of these materials in an ambient atmosphere. In the decomposition phase of the TGA curve for the ATPES functionalized silica, 44 AMU is the most prominent mass fragment lost. This mass is proposed to be the fragment of the surface group shown above the curve in Figure 4, -CH<sub>2</sub>CH<sub>2</sub>NH<sub>2</sub>. Since TGA-MS uses electron impact ionization, a hard ionization technique, it is not surprising that the whole surface group mass is not seen. The mass spectra data tracked for 44 AMU also shows a small spike at lower temperatures, trending with the desorption feature of the mass curve. This feature is likely adsorbed CO<sub>2</sub> being lost due to the low desorption temperature, although this conjecture has not been confirmed.

**Table 2.** Percent Conversion of Functional Groups on Silica Surface.

	Functional Group	Percent Conversion
ATPES		239*
AETS		101
2-CMTEs		111
HMT		206*
AAPT		151
TPMA		105
3-TPSA		259*

\*samples with an asterisk showed a clear excess of ligand on the surface.

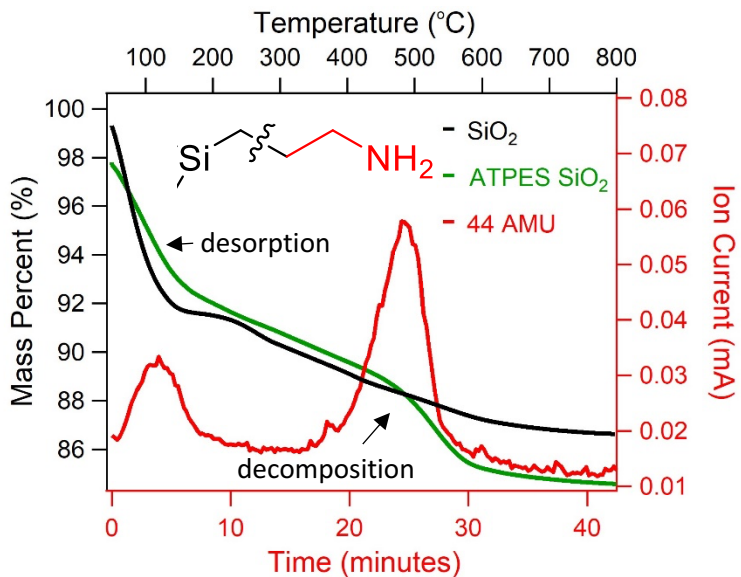


**Figure 4.** Thermogravimetric analysis data for  $1.0 \mu\text{m}$  bare silica (black) and ATPES functionalized silica (green) shown and MS-coupled mass curve data for the ATPES functionalized silica at mass fragment 44 AMU in red.

Seven functional groups were added to the surface of  $1 \mu\text{m}$  non-porous silica spheres and the ice nucleation activity was investigated. Frozen fraction data and  $n_s$  data can be seen in Figure 5, which shows limited difference between functional groups with this low ligand density (approx.  $1.6 \text{ per nm}^2$ ). AAPT, the amide functionalized group, showed slight decrease in activity compared to the non-functionalized silica resulting in the temperature of 50% frozen being two degrees lower than silica and fewer active sites at all temperatures. A slight increase over non-functionalized, non-porous spheres, is seen at lower temperatures ( $<-20.5$ ) for three samples, HMT, 3TPSA, and 2CMETS. These correspond to an alcohol, an ester, and a sulfone functional group, however these samples, based on TGA-MS, also had greater than a monolayer of surface

groups added to the surface. This result suggests that these groups partially reacted with themselves at the surface, which would create surface shape deformities and surface group density heterogeneities compared to the other samples. With the exception of these samples, none of the modified surfaces showed a large change in ice nucleation activity compared to the bare particles. These results are in contrast to work on organic monolayers which found that surface functional groups can play a significant role in activating ice nucleation, with carboxylic acids less effective ice nucleating particles than alcohols.<sup>46</sup>

Additional experiments were performed with the amine and carboxylic acid functionalized silica particles to see if charge on the ligand causes the minor differences in ice nucleation activity. Suspensions were prepared using solutions of NaOH (pH 11.5) or HCl (pH 3) to neutralize the charge of the amine and carboxylic acid respectively, with unique backgrounds for each trial to account for the added ions in the background water. Changing pH and therefore charge of these samples showed no effect on ice nucleation activity (Fig. S3). The addition of functional groups to amorphous silica has shown little effect on the immersion freezing temperatures. The minimal effects seen may be a result of the lack of ordering of functional groups at the surface with this low density compared to studies performed on monolayers. These samples are also on an amorphous particle rather than a crystalline one, which suggests that crystallinity plays a larger role in ice nucleation activity than surface groups, although further research is needed in this area. At such a low-density of surface groups on an amorphous substrate, it does not appear that there is an effect from acidity, oxidation, or number of heteroatoms on ice nucleation.

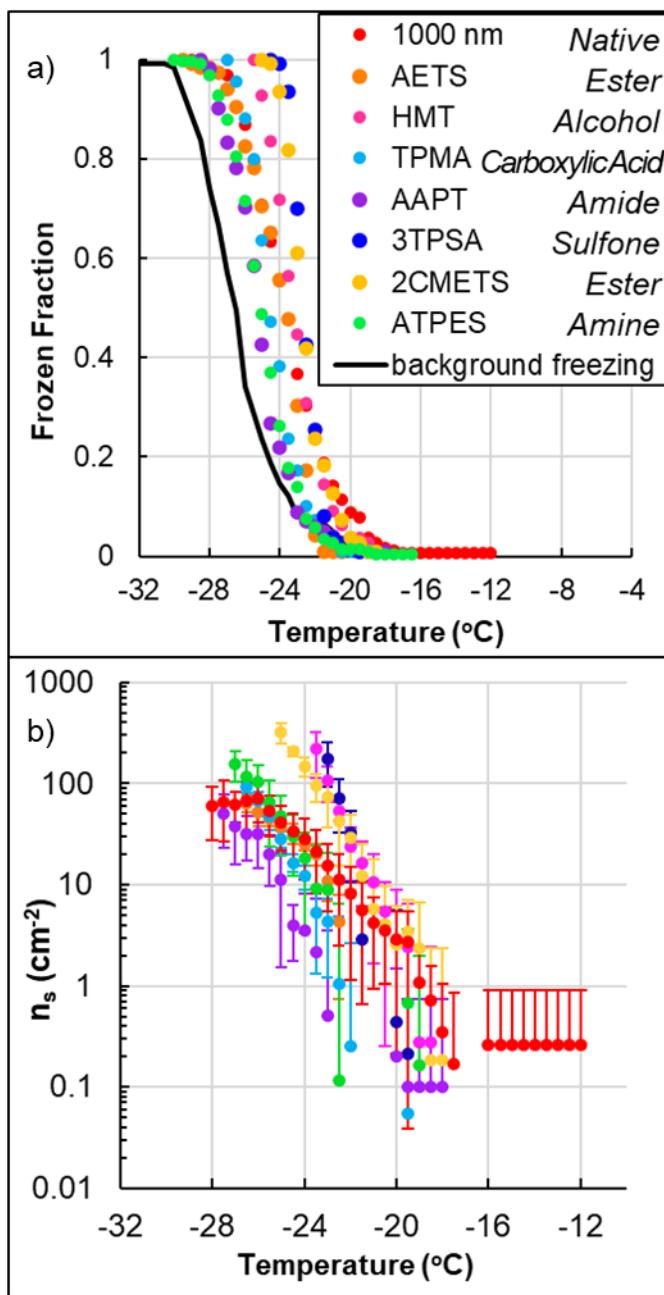


**Figure 5.** a) Functionalized silica frozen fraction data at a given temperature. b) Active sites per square centimeter ( $n_s$ ) for the same data with error across at least four trials. Both a and b use the same legend.

## Conclusions:

This work has helped to clarify the effects of porosity and crystallinity on ice nucleation in immersion mode freezing in the atmosphere. Many mineral dust particles as well as anthropogenic nanomaterials that are released into the atmosphere will have some porosity, which could be well-ordered or random. The crystallinity and surface features of solid aerosol particles are subject to change during their lifetime in the atmosphere. Atmospheric aging and processing can reduce the percent crystallinity, introduce surface defects, and chemically change the surface. Several silica samples, porous, non-porous and crystalline, were investigated as model heterogeneous ice nucleating particles in an immersion freezing chamber. The results show that quartz had the highest ice nucleation activity compared to other non-porous and porous samples. The porous samples have few active sites even with their larger surface area, suggesting that a pore alone may not be enough to act as an active site in immersion mode freezing. However future work could involve exploring other physical or chemical features that may be needed in a pore to make it an active site. It also suggests that crystallinity may be a more significant factor than porosity or functional groups for IN activity.

In addition to physical features, atmospheric aerosol can collect adsorbates and undergo chemical changes on their surfaces. This work has shown an example where low surface group density and ordering has very limited effects on heterogeneous ice nucleation at densities around 1.6 groups per square nm. In contrast, Qui et al. modeled that well-ordered monolayers with higher functional group densities (e.g. C<sub>30</sub>H<sub>61</sub>OH monolayers with 5.4 alcohols per square nm) of ligand can affect heterogeneous ice nucleation, with effects from chain lengths, rigidity and functional groups.<sup>46</sup> More work is needed to understand low density functionalized aerosol and non-ordered surface ligands affect ice nucleation, as these will also be present in the atmosphere.

The deconvolution of the effect of surface features, such as porosity, crystallinity, and surface functional groups, is key to a complete understanding of the aerosol contribution to ice formation in the troposphere, which influences climate and weather. Additionally, ice nucleation is significant in fields like materials science and agriculture, and as a result, this foundational understanding could have significance outside of atmospheric chemistry.

**Supporting Information:** contains characterization of non-porous silica spheres, dependence of ice nucleation activity on pH, and XRD of milled quartz samples.

## **Acknowledgements**

We acknowledge the assistance of Ekatarina Bazilevskaya and Gino Tambourine with BET data collection and TGA-MS respectively. We gratefully acknowledge support from NSF grant CHE-1904803.

## References:

- (1) Cziczo, D. J.; Froyd, K. D.; Hoose, C.; Jensen, E. J.; Diao, M.; Zondlo, M. A.; Smith, J. B.; Twohy, C. H.; Murphy, D. M. Clarifying the Dominant Sources and Mechanisms of Cirrus Cloud Formation. *Science* **2013**, *340* (6138), 1320–1324.
- (2) Hoose, C.; Möhler, O. Heterogeneous Ice Nucleation on Atmospheric Aerosols: A Review of Results from Laboratory Experiments. *Atmos. Chem. Phys.* **2012**, *12* (20), 9817–9854.
- (3) Zondlo, M. A.; Hudson, P. K.; Prenni, A. J.; Tolbert, M. A. Chemistry and Microphysics of Polar Stratospheric Clouds and Cirrus Clouds. *Annual Review of Physical Chemistry* **2000**, *51* (1), 473–499.
- (4) Murray, B. J.; O’Sullivan, D.; Atkinson, J. D.; Webb, M. E. Ice Nucleation by Particles Immersed in Supercooled Cloud Droplets. *Chem. Soc. Rev.* **2012**, *41* (19), 6519–6554.
- (5) Zhang, Z.; Liu, X.-Y. Control of Ice Nucleation: Freezing and Antifreeze Strategies. *Chem. Soc. Rev.* **2018**, *47* (18), 7116–7139.
- (6) Cox, S. J.; Kathmann, S. M.; Slater, B.; Michaelides, A. Molecular Simulations of Heterogeneous Ice Nucleation. I. Controlling Ice Nucleation through Surface Hydrophilicity. *J. Chem. Phys.* **2015**, *142* (18), 184704.
- (7) Jin, J.; Yurkow, E. J.; Adler, D.; Lee, T.-C. Improved Freeze Drying Efficiency by Ice Nucleation Proteins with Ice Morphology Modification. *Food Research International* **2018**, *106*, 90–97.
- (8) Kobayashi, A.; Horikawa, M.; Kirschvink, J. L.; Golash, H. N. Magnetic Control of Heterogeneous Ice Nucleation with Nanophase Magnetite: Biophysical and Agricultural Implications. *PNAS* **2018**, *115* (21), 5383–5388.
- (9) Vali, G.; DeMott, P. J.; Möhler, O.; Whale, T. F. Technical Note: A Proposal for Ice Nucleation Terminology. *Atmospheric Chemistry and Physics* **2015**, *15* (18), 10263–10270.
- (10) Vali, G. Ice Nucleation — a Review. In *Nucleation and Atmospheric Aerosols* 1996; Elsevier, 1996; pp 271–279.
- (11) Kärcher, B.; Lohmann, U. A Parameterization of Cirrus Cloud Formation: Heterogeneous Freezing. *Journal of Geophysical Research: Atmospheres* **2003**, *108* (D14).
- (12) de Boer, G.; Hashino, T.; Tripoli, G. J. Ice Nucleation through Immersion Freezing in Mixed-Phase Stratiform Clouds: Theory and Numerical Simulations. *Atmospheric Research* **2010**, *96* (2), 315–324.
- (13) Lupi, L.; Peters, B.; Molinero, V. Pre-Ordering of Interfacial Water in the Pathway of Heterogeneous Ice Nucleation Does Not Lead to a Two-Step Crystallization Mechanism. *J. Chem. Phys.* **2016**, *145* (21), 211910.
- (14) Fitzner, M.; Pedevilla, P.; Michaelides, A. Predicting Heterogeneous Ice Nucleation with a Data-Driven Approach. *Nat Commun* **2020**, *11* (1), 4777.
- (15) Hiranuma, N.; Hoffmann, N.; Kiselev, A.; Dreyer, A.; Zhang, K.; Kulkarni, G.; Koop, T.; Möhler, O. Influence of Surface Morphology on the Immersion Mode Ice Nucleation Efficiency of Hematite Particles. *Atmos. Chem. Phys.* **2014**, *14* (5), 2315–2324.
- (16) Kanji, Z. A.; Sullivan, R. C.; Niemand, M.; DeMott, P. J.; Prenni, A. J.; Chou, C.; Saathoff, H.; Möhler, O. Heterogeneous Ice Nucleation Properties of Natural Desert Dust Particles Coated with a Surrogate of Secondary Organic Aerosol. *Atmospheric Chemistry and Physics* **2019**, *19* (7), 5091–5110.
- (17) Kulkarni, G.; Zhang, K.; Zhao, C.; Nandasiri, M.; Shutthanandan, V.; Liu, X.; Fast, J.; Berg, L. Ice Formation on Nitric Acid-Coated Dust Particles: Laboratory and Modeling Studies. *J Geophys Res Atmos.* **2015**, *120* (15), 7682–7698.
- (18) Chong, E.; King, M.; Marak, K. E.; Freedman, M. A. The Effect of Crystallinity and Crystal Structure on the Immersion Freezing of Alumina. *J. Phys. Chem. A* **2019**, *123* (12), 2447–2456.

(19) Kiselev, A.; Bachmann, F.; Pedevilla, P.; Cox, S. J.; Michaelides, A.; Gerthsen, D.; Leisner, T. Active Sites in Heterogeneous Ice Nucleation—the Example of K-Rich Feldspars. *Science* **2017**, *355* (6323), 367–371.

(20) Holden, M. A.; Whale, T. F.; Tarn, M. D.; O’Sullivan, D.; Walshaw, R. D.; Murray, B. J.; Meldrum, F. C.; Christenson, H. K. High-Speed Imaging of Ice Nucleation in Water Proves the Existence of Active Sites. *Science Advances* **2019**, *5* (2),

(21) Holden, M. A.; Campbell, J. M.; Meldrum, F. C.; Murray, B. J.; Christenson, H. K. Active Sites for Ice Nucleation Differ Depending on Nucleation Mode. *PNAS* **2021**, *118* (18).

(22) Friddle, R. W.; Thürmer, K. How Nanoscale Surface Steps Promote Ice Growth on Feldspar: Microscopy Observation of Morphology-Enhanced Condensation and Freezing. *Nanoscale* **2019**, *11* (44), 21147–21154.

(23) Jiang, J.; Li, G. X.; Sheng, Q.; Tang, G. H. Microscopic Mechanism of Ice Nucleation: The Effects of Surface Rough Structure and Wettability. *Applied Surface Science* **2020**, *510*, 145520.

(24) Chong, E.; Marak, K. E.; Li, Y.; Freedman, M. A. Ice Nucleation Activity of Iron Oxides via Immersion Freezing and an Examination of the High Ice Nucleation Activity of FeO. *Phys. Chem. Chem. Phys.* **2021**, *23* (5), 3565–3573.

(25) Schill, G. P.; Tolbert, M. A. Depositional Ice Nucleation on Monocarboxylic Acids: Effect of the O:C Ratio. *J. Phys. Chem. A* **2012**, *116* (25), 6817–6822.

(26) Marcolli, C. Deposition Nucleation Viewed as Homogeneous or Immersion Freezing in Pores and Cavities. *Atmospheric Chemistry and Physics* **2014**, *14* (4), 2071–2104.

(27) David, R. O.; Marcolli, C.; Fahrni, J.; Qiu, Y.; Perez Sirk, Y. A.; Molinero, V.; Mahrt, F.; Brühwiler, D.; Lohmann, U.; Kanji, Z. A. Pore Condensation and Freezing Is Responsible for Ice Formation below Water Saturation for Porous Particles. *Proceedings of the National Academy of Sciences* **2019**, *116* (17), 8184–8189.

(28) Moore, E. B.; Llave, E. de la; Welke, K.; Scherlis, D. A.; Molinero, V. Freezing, Melting and Structure of Ice in a Hydrophilic Nanopore. *Phys. Chem. Chem. Phys.* **2010**, *12* (16), 4124–4134.

(29) David, R. O.; Fahrni, J.; Marcolli, C.; Mahrt, F.; Brühwiler, D.; Kanji, Z. A. The Role of Contact Angle and Pore Width on Pore Condensation and Freezing. *Atmospheric Chemistry and Physics* **2020**, *20* (15), 9419–9440.

(30) Wagner, R.; Kiselev, A.; Möhler, O.; Saathoff, H.; Steinke, I. Pre-Activation of Ice-Nucleating Particles by the Pore Condensation and Freezing Mechanism. *Atmospheric Chemistry and Physics* **2016**, *16* (4), 2025–2042.

(31) Aylmore, L. a. G.; Quirk, J. P. The Micropore Size Distributions of Clay Mineral Systems. *Journal of Soil Science* **1967**, *18* (1), 1–17.

(32) Alstadt, V. J.; Dawson, J. N.; Losey, D. J.; Sihvonen, S. K.; Freedman, M. A. Heterogeneous Freezing of Carbon Nanotubes: A Model System for Pore Condensation and Freezing in the Atmosphere. *J. Phys. Chem. A* **2017**, *121* (42), 8166–8175.

(33) Kittaka, S.; Ueda, Y.; Fujisaki, F.; Iiyama, T.; Yamaguchi, T. Mechanism of Freezing of Water in Contact with Mesoporous Silicas MCM-41, SBA-15 and SBA-16: Role of Boundary Water of Pore Outlets in Freezing. *Phys. Chem. Chem. Phys.* **2011**, *13* (38), 17222–17233.

(34) Morishige, K.; Kawano, K. Freezing and Melting of Water in a Single Cylindrical Pore: The Pore-Size Dependence of Freezing and Melting Behavior. *The Journal of Chemical Physics* **1999**, *110* (10), 4867–4872.

(35) Li, C.; Tao, R.; Luo, S.; Gao, X.; Zhang, K.; Li, Z. Enhancing and Impeding Heterogeneous Ice Nucleation through Nanogrooves. *J. Phys. Chem. C* **2018**, *122* (45), 25992–25998.

(36) Pach, E.; Verdaguer, A. Pores Dominate Ice Nucleation on Feldspars. *J. Phys. Chem. C* **2019**, *123* (34), 20998–21004.

(37) Whale, T. F.; Rosillo-Lopez, M.; Murray, B. J.; Salzmann, C. G. Ice Nucleation Properties of Oxidized Carbon Nanomaterials. *J. Phys. Chem. Lett.* **2015**, *6* (15), 3012–3016.

(38) Toney, M. F.; Howard, J. N.; Richer, J.; Borges, G. L.; Gordon, J. G.; Melroy, O. R.; Wiesler, D. G.; Yee, D.; Sorensen, L. B. Voltage-Dependent Ordering of Water Molecules at an Electrode–Electrolyte Interface. *Nature* **1994**, *368* (6470), 444–446.

(39) Ehre, D.; Lavert, E.; Lahav, M.; Lubomirsky, I. Water Freezes Differently on Positively and Negatively Charged Surfaces of Pyroelectric Materials. *Science* **2010**, *327* (5966), 672–675.

(40) Schwidetzky, R.; Sun, Y.; Fröhlich-Nowoisky, J.; Kunert, A. T.; Bonn, M.; Meister, K. Ice Nucleation Activity of Perfluorinated Organic Acids. *J. Phys. Chem. Lett.* **2021**, *12* (13), 3431–3435.

(41) Yang, H.; Ma, C.; Li, K.; Liu, K.; Loznik, M.; Teeuwen, R.; van Hest, J. C. M.; Zhou, X.; Herrmann, A.; Wang, J. Tuning Ice Nucleation with Supercharged Polypeptides. *Advanced Materials* **2016**, *28* (25), 5008–5012.

(42) Glatz, B.; Sarupria, S. The Surface Charge Distribution Affects the Ice Nucleating Efficiency of Silver Iodide. *J. Chem. Phys.* **2016**, *145* (21), 211924.

(43) Lupi, L.; Molinero, V. Does Hydrophilicity of Carbon Particles Improve Their Ice Nucleation Ability? *J. Phys. Chem. A* **2014**, *118* (35), 7330–7337..

(44) Pedevilla, P.; Fitzner, M.; Michaelides, A. What Makes a Good Descriptor for Heterogeneous Ice Nucleation on OH-Patterned Surfaces. *Phys. Rev. B* **2017**, *96* (11), 115441.

(45) Gavish, M.; Popovitz-Biro, R.; Lahav, M.; Leiserowitz, L. Ice Nucleation by Alcohols Arranged in Monolayers at the Surface of Water Drops. *Science* **1990**, *250* (4983), 973–975.

(46) Qiu, Y.; Odendahl, N.; Hudait, A.; Mason, R.; Bertram, A. K.; Paesani, F.; DeMott, P. J.; Molinero, V. Ice Nucleation Efficiency of Hydroxylated Organic Surfaces Is Controlled by Their Structural Fluctuations and Mismatch to Ice. *J. Am. Chem. Soc.* **2017**, *139* (8), 3052–3064.

(47) DeMott, P.; Mason, R.; McCluskey, C.; Hill, T. C.; Perkins, R.; Desyaterik, Y.; Bertram, A.; Trueblood, J.; Grassian, V.; Qiu, Y.; et al. Ice Nucleation by Particles Containing Long-Chain Fatty Acids of Relevance to Freezing by Sea Spray Aerosols. *Environmental Science: Processes & Impacts* **2018**, *20* (11), 1559–1569.

(48) Ochshorn, E.; Cantrell, W. Towards Understanding Ice Nucleation by Long Chain Alcohols. *J. Chem. Phys.* **2006**, *124* (5), 054714.

(49) Zobrist, B.; Koop, T.; Luo, B. P.; Marcolli, C.; Peter, T. Heterogeneous Ice Nucleation Rate Coefficient of Water Droplets Coated by a Nonadecanol Monolayer. *J. Phys. Chem. C* **2007**, *111* (5), 2149–2155.

(50) Pluhařová, E.; Vrbka, L.; Jungwirth, P. Effect of Surface Pollution on Homogeneous Ice Nucleation: A Molecular Dynamics Study. *J. Phys. Chem. C* **2010**, *114* (17), 7831–7838.

(51) Atre, S. V.; Liedberg, B.; Allara, D. L. Chain Length Dependence of the Structure and Wetting Properties in Binary Composition Monolayers of OH- and CH<sub>3</sub>-Terminated Alkanethiolates on Gold. *Langmuir* **1995**, *11* (10), 3882–3893.

(52) Allara, D. L. Critical Issues in Applications of Self-Assembled Monolayers. *Biosensors and Bioelectronics* **1995**, *10* (9), 771–783.

(53) Zhu, Z.; Xiang, J.; Wang, J.; Qiu, D. Effect of Polyvinyl Alcohol on Ice Formation in the Presence of a Liquid/Solid Interface. *Langmuir* **2017**, *33* (1), 191–196.

(54) Zender, C. S.; Miller, R. L. R. L.; Tegen, I. Quantifying Mineral Dust Mass Budgets: Terminology, Constraints, and Current Estimates. *Eos, Trans. Amer. Geophys. Union* **2004**, *85* (48), 509–512.

(55) Boose, Y.; Welti, A.; Atkinson, J.; Ramelli, F.; Danielczok, A.; Bingemer, H. G.; Plötze, M.; Sierau, B.; Kanji, Z. A.; Lohmann, U. Heterogeneous Ice Nucleation on Dust Particles Sourced from Nine Deserts Worldwide – Part 1: Immersion Freezing. *Atmospheric Chem. Phys.* **2016**, *16* (23), 15075–15095..

(56) Schill, G. P.; Genareau, K.; Tolbert, M. A. Deposition and Immersion-Mode Nucleation of Ice by Three Distinct Samples of Volcanic Ash. *Atmospheric Chem. Phys* **2015**, *15* (13), 7523–7536.

(57) Kumar, A.; Marcolli, C.; Peter, T. Ice Nucleation Activity of Silicates and Aluminosilicates in Pure Water and Aqueous Solutions – Part 2: Quartz and Amorphous Silica. *Atmospheric Chemistry and Physics* **2019**, *19* (9), 6035–6058.

(58) Chernoff, D. I.; Bertram, A. K. Effects of Sulfate Coatings on the Ice Nucleation Properties of a Biological Ice Nucleus and Several Types of Minerals. *J Geophys Res Atmos* **2010**, *115* (D20).

(59) Kaufmann, L.; Marcolli, C.; Hofer, J.; Pinti, V.; Hoyle, C. R.; Peter, T. Ice Nucleation Efficiency of Natural Dust Samples in the Immersion Mode. *Atmospheric Chemistry and Physics* **2016**, *16* (17), 11177–11206.

(60) Harrison, A. D.; Lever, K.; Sanchez-Marroquin, A.; Holden, M. A.; Whale, T. F.; Tarn, M. D.; McQuaid, J. B.; Murray, B. J. The Ice-Nucleating Ability of Quartz Immersed in Water and Its Atmospheric Importance Compared to K-Feldspar. *Atmospheric Chemistry and Physics* **2019**, *19* (17), 11343–11361.

(61) Wang, X.; Zhang, Y.; Luo, W.; Elzatahry, A. A.; Cheng, X.; Alghamdi, A.; Abdullah, A. M.; Deng, Y.; Zhao, D. Synthesis of Ordered Mesoporous Silica with Tunable Morphologies and Pore Sizes via a Nonpolar Solvent-Assisted Stöber Method. *Chem. Mater.* **2016**, *28* (7), 2356–2362.

(62) Cash, B. M.; Wang, L.; Benicewicz, B. C. The Preparation and Characterization of Carboxylic Acid-Coated Silica Nanoparticles. *J Polym Sci Part A: Polym Chem* **2012**, *50*, 2533–2540.

(63) Mahalingam, V.; Onclin, S.; Pe’ter, M.; Jan Ravoo, B.; Huskens, J.; Reinoudt, D. N. Directed Self-Assembly of Functionalized Silica Nanoparticles on Molecular Printboards through Multivalent Supramolecular Interactions. *Langmuir* **2004**, *20* (26), 11756–11762.

(64) Zhuravlev, L. T. The Surface Chemistry of Amorphous Silica. Zhuravlev Model. *Colloids Surf. A* **2000**, *173*, 1–38.

(65) D’Souza, A. S.; Pantano, C. G.; Kallury, K. M. R. Determination of the Surface Silanol Concentration of Amorphous Silica Surfaces Using Static Secondary Ion Mass Spectroscopy. *J. Vac. Sci. Technol. A* **1997**, *15* (3), 526–531.

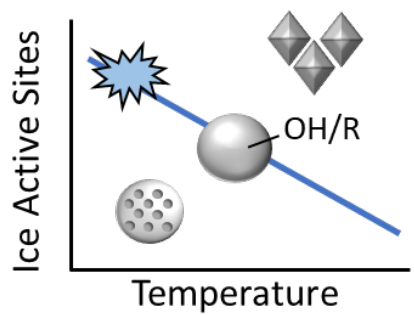
(66) O’Sullivan, D.; Murray, B. J.; Ross, J. F.; Whale, T. F.; Price, H. C.; Atkinson, J. D.; Umo, N. S.; Webb, M. E. The Relevance of Nanoscale Biological Fragments for Ice Nucleation in Clouds. *Scientific Reports* **2015**, *5*, 8082.

(67) Vali, G. Quantitative Evaluation of Experimental Results on the Heterogeneous Freezing Nucleation of Supercooled Liquids. *J. Atmos. Sci.* **1971**, *28* (3), 402–409.

(68) Zimmermann, F.; Weinbruch, S.; Schütz, L.; Hofmann, H.; Ebert, M.; Kandler, K.; Worringen, A. Ice Nucleation Properties of the Most Abundant Mineral Dust Phases. *J Geophys Res Atmos.* **2008**, *113* (D23).

(69) Shaw, S. A.; Jim Hendry, M. Geochemical and Mineralogical Impacts of H<sub>2</sub>SO<sub>4</sub> on Clays between PH 5.0 and –3.0. *Appl Geochem.* **2009**, *24* (2), 333–345.

(70) Zobrist, B.; Marcolli, C.; Peter, T.; Koop, T. Heterogeneous Ice Nucleation in Aqueous Solutions: The Role of Water Activity. *J. Phys. Chem. A* **2008**, *112* (17), 3965–3975.



TOC Graphic